Università degli Studi di Ferrara

DOTTORATO DI RICERCA IN
Scienze dell'ingegneria

CICLO XXIII

COORDINATORE Prof. Trillo Stefano

SHAPE MEMORY
ACTUATOR:THERMOMECHANICAL TRAINING AND
SURFACE OPTIMIZATION OF SHAPE MEMORY WIRES
EMBEDDED IN A POLYMERIC MATRIX

Settore Scientifico Disciplinare ING-IND/21

Dottorando	**Tutore**
Dott. Scoponi Martina	Prof. Garagnani Gian Luca
_____	_____
(firma)	*(firma)*

Anni 2008/2010

INDEX

ABSTRACT

In the first part of my work I studied the mechanical and thermal behaviour of NiTi wires and strips in order to find the best training cycle to achieve a good compromise between transformation temperatures, recovery forces and phase reversibility. Other parameters such as the stress-rate and maximum recovery deformations, useful to realize smart composites, were evaluated. DSC and DMTA analyses were performed on NiTi thin strips that were cold rolled with different thickness reductions. DSC is a well-known technique used to find the transformation temperatures of SMAs. Contrary to DSC, DMTA is not a traditional characterization method for shape memory alloys. Therefore, in this work I tried to find a correlation between the results of DSC and DMTA analysis, according to different hardenings induced by cold rolling.

In the second part I dealt with the interface bonding optimization between polymer matrices and NiTi wires. Smart composites take advantage of the adhesion between the NiTi wires and the polymer matrix. Their mechanical properties depend strongly on the efficiency of stresses and deformations transfer at the interface between the wires and the surrounding matrix. This way, adhesion must be improved to avoid the degradation or premature failure of the actuation. I focused on the evaluation of the interface strength between NiTi wires and two kinds of thermosetting resins: polyester and vinylester. Different surface treatments were performed on the NiTi wires in order to increase the performance of the wire-resin interface adhesion. In particular, chemical passivation by using acid solution and functionalization by using silane coupling agents, were considered. Pull-out tests were carried out to quantify the improvement of the interface adhesion.

Moreover, during my PhD I also dealt with the theoretical modeling of SMA materials and the mechanical behavior of smart composites during activation, but this topic is not discussed in this thesis.

SOMMARIO

Nella prima parte del mio lavoro sono stati studiati il comportamento termico e meccanico di file e lamine a memoria di forma per trovare il ciclaggio migliore per ottenere un buon compromesso tra temperature di trasformazione, forze di recupero e reversibilità della trasformazione martensitica. Anche altri parametri sono stati valutati, come la velocità di applicazione dello sforzo e la massima deformazione recuperabile, utili per dimensionare un composito funzionale. Sono state utilizzate in questa fase prove DSC e DMTA su lamine NiTi sottoposte a laminazione con differenti riduzioni di spessore. L'analisi DSC è una tecnica nota per analizzare le temperature di trasformazione di fase, mentre la DMTA è una tecnica che tradizionalmente non viene usata per lo studio e la caratterizzazione delle leghe a memoria di forma. Perciò in questo lavoro si è cercato di trovare una correlazione tra i risultati dell'analisi DSC e DMTA in base all'incrudimento provocato dalla laminazione.

Nella seconda parte di questo lavoro è stata trattata l'ottimizzazione del legame di interfaccia tra le matrici polimeriche e i fili NiTi. I compositi funzionali devono il loro funzionamento all'adesione tra i fili NiTi e la matrice polimerica. Le loro proprietà meccaniche dipendono fortemente dall'efficienza nel trasferire sforzi e deformazioni che si generano all'interfaccia tra i fili e la matrice. In questa fase il lavoro si è concentrato sulla resistenza dell'interfaccia tra i fili NiTi e due diverse resine termoindurenti: poliestere e vinilestere. Sui fili sono stati effettuati diversi trattamenti per aumentare l'adesione. In particolare sono stati presi in considerazioni trattamenti di passivazione chimica con soluzioni acide e funzionalizzazione con agenti silanizzanti. Per quantificare l'efficacia dei trattamenti sono state effettuate prove di pull-out.

Inoltre durante il mio dottorato mi sono anche occupata di modellazione teorica dei materiali a memoria di forma e del comportamento meccanico dei composite funzionali durante l'attivazione, ma questi argomenti non sono riportati in questo lavoro.

PREFACE

The research activity I carried out during my PhD is the result of three years' study at the University of Ferrara, Italy, from January 2008 to December 2010. Professor Gian Luca Garagnani was my main supervisor.

During my PhD, I focused on the study of shape memory alloys, in particular NiTi alloys. These interesting alloys are successfully used in several mechanical devices, replacing expensive and cumbersome mechanical systems. NiTi alloys have the potential to be used in the design of actuators, sensors and, especially, functional structures, in which they are directly or indirectly embedded in a polymer matrix. In these applications the ability of NiTi wires or strips to generate large recovery stresses is used.

Most of the research activity is presented here as a collection of two articles. Each paper is an individual piece of work with separate sections including: abstract, introduction, results and discussion, conclusion and references. The manuscripts are:

Article 1:

M. MERLIN, M. SCOPONI, "Using DSC and DMTA for the study of thermo-mechanical treatments improving the transformational behavior of Ti-rich nitinol sheets" International Journal of Materials Engineering and Technology, 4-1, 2010, p.49-61.

Article 2:

M. MERLIN, M. SCOPONI, C. SOFFRITTI, "On the improved adhesion of NiTi wires embedded in polyster and vinylester resins", preprint, 2011.

The thesis is organized as follows: in the section "Introduction" are presented the main aspects of NiTi shape memory alloys and an overview of the most important smart actuators in which SMAs are embedded in composite matrices. In the next section "Articles" are collected the following manuscripts: "Article 1" is reported in the same format it was published, while "Article 2" is reported in a preprint version.

INTRODUCTION

1.1. Shape Memory Materials

The name Shape Memory Materials refers to the ability to remember a shape either by applying stress or by increasing the temperature. Even after high strain, shape memory materials can recover the geometry previously memorized (during their manufacturing).

These materials can be alloys, polymers and also ceramics, however, the shape memory effect was first observed in NiTi alloys. Shape memory alloys based on NiTi (53.57 w/o Ni) were first investigated by the Naval Ordnance Laboratory, hence they are referred to as NITINOL.

The shape memory alloys can behave in three different ways:

1. One way shape memory effect (OWSME): the material, plastically deformed in the low temperature martensitic phase, can be restored to its original shape configuration by heating above a critical temperature.

2. Two way shape memory effect (TWSME): the material remembers both the high and low temperature configuration.

3. Superelasticity: the material can be subjected to high deformation in the austenitic phase and then completely recovers after the load has been removed.

These three behaviors are possible thanks to a geometrical transformation that is completely reversible and occurs between a high temperature stable phase (austenite) and a low temperature stable phase (martensite). The mechanical proprieties of these alloys depend on the content of these two phases, i.e. the temperature or stress applied.

The shape memory effect is based on the transformation from martensite (or γ phase) to austenite (or α phase) and vice versa. martensitic transformations are diffusionless, the change in the crystal structure being achieved by a deformation of the parent phase austenite, which occurs with a crystallographic change in the alloy but without volume change.

This transformation occurs with thermal hysteresis: the parent phase begins to transform into twinned martensite at the martensitic start temperature (Ms) and completes transformation to martensite at the martensitic finish temperature (Mf). When the transformation is complete the

material is completely in the twinned martensitic phase, which is also called self-accommodated martensite: this γ→α transformation occurs by the formations of twins inside the austenitic lattice. Similarly, during heating, the reverse transformation initiates at the austenitic start temperature (As) and the transformation is completed at the austenitic finish temperature (Af). There are two crystallographic constrains that rule the martensitic transformation:

1. During transformation there is a fixed plane called the "habit plane" that is not subject to deformation or rotation. On this plane the martensite begins its nucleation and the transformation is a slip on a parallel plane.

2. austenite and martensite have two different lattices, the first is FCC (Face-Centered Cubic) and the second is a BCT (Body-Centered Tetragonal) or a BCC (Body-Centered Cubic).

There is a similarity between the two lattices and, moreover, the transformation of the FCC austenite in martensite could be seen as a normal stress, a shear stress and a rotation on the habit plane. Figure 1.1 shows the martensitic transformation mechanisms.
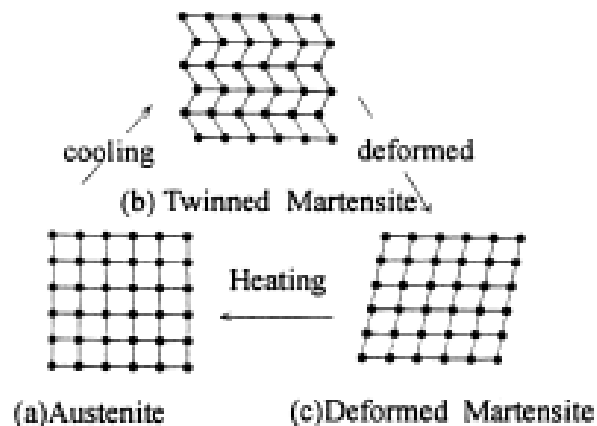
Figure 1.1: Shape Memory Effect [1].

The unique behavior of NiTi is based on the temperature-dependent austenite-to-martensite phase transformation on an atomic scale, which is also called thermoelastic martensitic transformation. The thermoelastic martensitic transformation causing the shape recovery is a

result of the need of the crystal lattice structure to accommodate to the minimum energy state for a given temperature [1].

The reversibility of the martensitic transformation is possible because there is a definite orientation relationship during the change in phase because the atoms have to move in a coordinated manner. A typical feature of martensitic transformations is that each colony of martensite laths/plates consists of a stack in which different variants alternate (twinning). This allows large shears to be accommodated with minimal macroscopic shear.

At the end of the transformation the microstructure will have a twinned plate-like morphology with the martensite variant pointing in a different direction from the parent phase. If shear stress is applied, the boundaries of twinned martensite will point in the load direction with a mechanism called detwinning. In figure 1 this mechanism is shown by the transition from configuration (b) to (c). During heating austenite nucleation will occur on the martensite plates according to the same crystallographic relation on the inverse transformation.

1.2. Thermo-mechanical behavior

The mechanical properties of shape memory alloys depend on the temperature related to the transformation temperatures.

If T<Mf the material will be completely in the martensitic phase. In figure 2 the mechanical behavior of the multi-variant martensite in a NiTi alloy is shown. There are three different regions recognizable in the stress-strain curve; the first one is a linear σ-ε relation, if the applied load is removed the strain is completely recovered. The second region starts when it has reached critical tension σ_S^{CR} after which the detwinning of martensite takes place. When the twin boundaries point towards the applied load and are under constant stress, it is possible to have considerable deformation.

The third zone begins at critical stress and after detwinning there is another elastic region of the single-variant martensite.

If the external load is removed before σ_F^{CR} it is possible to recover the shape completely by heating the material to a temperature T>Af, the maximum deformation recoverable is named ε_L (see figure 1.2).
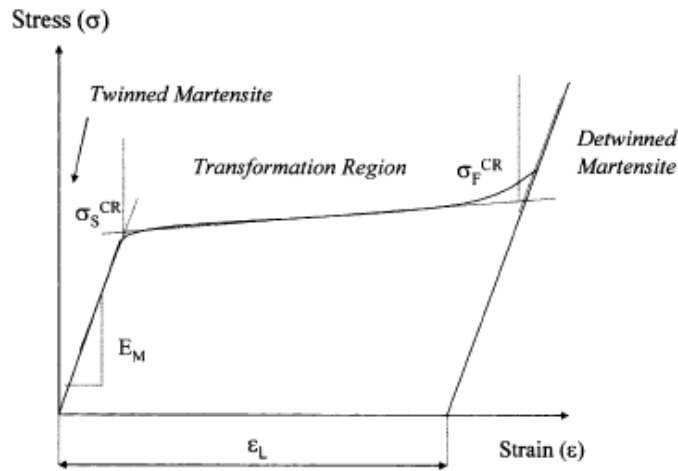
Figure 1.2: Stress-strain curve for shape memory alloys in martensitic phase [1].

If the material is in the austenitic phase it is possible to see the first elastic region as well as a region in which the deformation occurs under a constant stress, however, the austenite has a higher modulus and different values for σ_{SCR}, σ_{FCR} e di ε_L. In figure 3, the curves have stress-strain at different temperatures: (a) T>Af, the behavior is superelastic . In the OA line the slope is the austenite modulus, in the AB line martensitic transformation occurs under an applied load and the material can undergo high strain with constant stress and in this case the martensite is a single-variant.

When unloading along the BC line, the behaviour is linear. In the CD line the inverse transformation occurs and it is possible to recover the strain of the AB line. The last part of the curve DO returns to the initial configuration.

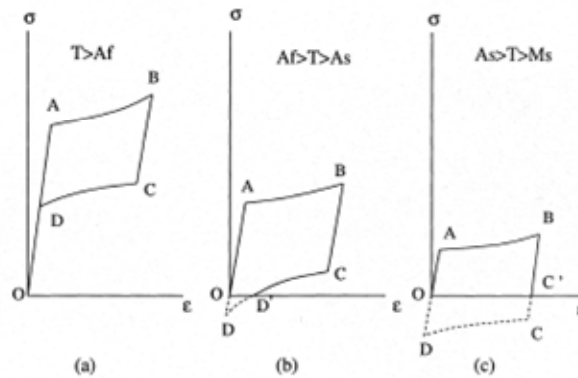Figure 1.3 (b) and (c) show the behavior at intermediate temperature values.

Figure 1.3: Temperature dependent behaviour of shape memory alloys [1].

1.3 Applications of Shape Memory Alloys

The most well-known shape memory alloys are NiTi based. There are binary or ternary alloys in which there is also Cu and they have different properties that make it possible to have custom made alloys for a range of specific applications.
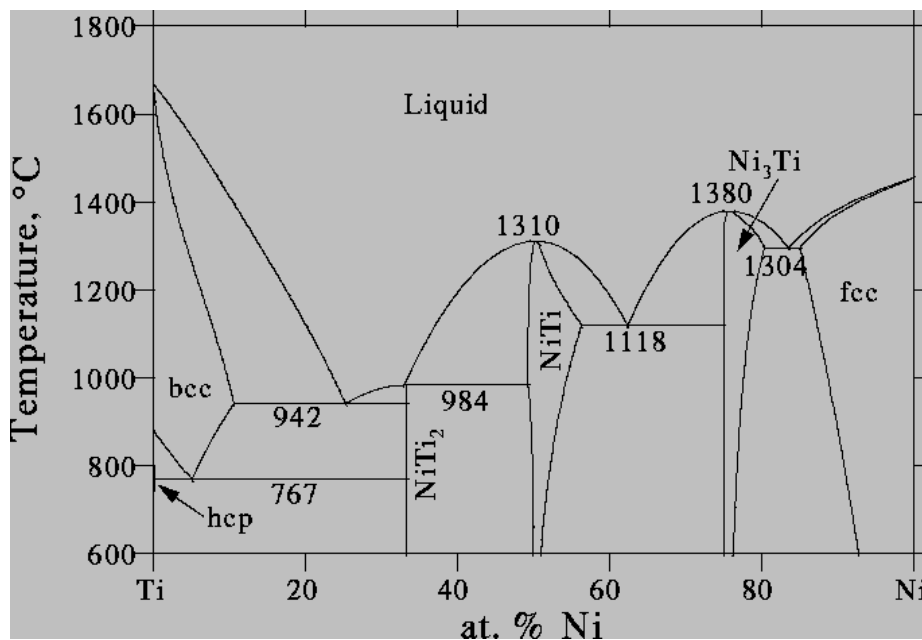

Figure 1.4: State diagram of NiTi alloys [1].

The NiTi alloys have an equi-atomic composition, making it possible to add Ni or Ti or other elements due to good solubility, which is shown in figure 1.4 in the state diagrams of a binary NiTi alloy.

By increasing or decreasing the Ni content, the transformation temperature could also be changed, therefore, high Ni content is preferred for biomedical applications in order to have $Af<T_{amb}$; a high Ni content also increases the yield resistance of the austenite

Other chemical elements present in the NiTi alloys could be Fe and Cr to decrease the transformation temperatures and Cu to decrease the thermal hysteresis and the martensite modulus.

Cold hardening combined with a thermal treatment can lead to the two-way shape memory effect but this effect is subject to fatigue and diminishes after frequent activation.

The fabrication of the alloy is influenced by the high oxygen reactivity of Titanium and all the melting processes must be done in an inert atmosphere. However, after solidification, the alloy can be subjected to either cold or hot working without oxidation.

During cold working, annealing is necessary to make sure the material is not hardened so much that the shape memory effect is reduced. Wire-drawing is the most common technique and this also explains why the most common commercial shapes are strips with variable thickness and wires with small diameters.

The thermal treatment to memorize the shape in the austenitic phase is generally performed at 500-800°C for several minutes and the sample is kept constrained in the chosen configuration.

Strains of 8% can be completely recovered by heat transformation from the deformed martensitic phase to the austenitic phase. If the material is constrained from recovering its memorized shape, high stresses of up to 700 MPa can be induced.

SMA used as embedded actuators would typically take the form of plastically-elongated wires constrained from recovering their normal memorized length during fabrication in order to exploit the good weight/strength ratio.

1.4 Actuators

Actuators are used in applications in which it is essential to control processes and they could be used for biomedical, mechanical and aerospace purposes.

They could be defined as a link between the information which controls a process and the process itself.

In many cases, the actuator is electrically activated, but there are also other kinds of actuators with optical, magnetic, fluid-dynamic or piezoelectric characteristics.

SMAs have mostly been used as thermal actuators, where the temperature gradient is the driving force of phase transformation and the corresponding change in microstructure provides the necessary displacement and/or force.

Furthermore, SMAs could also be used for microactuator applications thanks to their weight/strength ratio that allows small devices to be built which are also capable of high recovery forces. Their working is based on the one-way shape memory effect and this could be used to generate a force, a displacement or both. The actuation is often made through heating by means of Joule effect.

There are three possible uses for the SMA actuators:

1. Free recovery: without an external load the SMA device returns to the original configuration when T>Af.

2. Constraint recovery: if the device has a pre-strain but is not free to recover it, a high force is generated.

3. Energy production: when the force generated during the transformation is higher than an external load and produces work. When the component cools down, the external force is higher.

The third configuration is the most common and the force and displacement could also be varied according to the mechanism chosen. When the load is in tension or compression only, small displacements could be achieved, while with flexural or torsional loads the displacements are bigger.

After initial research on SMA actuators, they have mostly been commercialized as glass frames, cell phone antennae and in biomedical applications (stents, braces, etc.). These applications take

advantage of their superelasticity behavior. The actuators used are springs or wires, as well as strips, and the new trend is heading towards miniactuators built as sputtered films.

Table 1.1 reports the most commonly used actuators with SMA materials. The constrained recovery is used in many electrical applications in which the good connection is realised by a force-free link.

The thermal actuators used to generate work are often made of an SMA spring connected to another passive spring and, in these cases, the actuators control both the temperature and the fluid.

The problem in electrical applications is the high resistivity that needs high power to heat the SMA device, so that prototypes have only been developed in robotic applications.

The actuators discussed above can be considered as parts of smart structures; the actuation function is performed by discrete SMA elements. The SMA elements can also be easily integrated into matrix materials and yielding smart or adaptive materials. In comparison with alternative 'actuating' or 'sensing' materials, SMAs offer several important advantages and extra possibilities: (i) much larger reversible strains (up to 8%), (ii) ability to generate extremely high stresses (up to 800 MPa), (iii) large reversible changes of mechanical and physical characteristics, (iv) high damping capacity, and (v) ability to generate stresses and strains gradually.

Table 1.1: Example of SMA actuators.

Shape Memory Effect	Mechanism	Applications
One Way SME	Thermal activation and constrained recovery	Joints Electrical connections
One Way SME	Thermal activation and work production with passive mechanism	Safety valves Air conditioners Electrical switches Thermal switches
One Way SME	Electrical activation and work production with passive mechanism	Control system for lightening Grippers

Therefore, many experts believe that SMAs offer very promising prospects in this new, rapidly evolving field of material research. The rapidly increasing interest in these materials is also due to the fact thin SMA wires can be easily embedded into advanced structural materials, such as polymer matrix composites, without losing the structural integrity of the matrix material. By embedding shape memory elements into a polymer matrix or polymer matrix composite, novel material characteristics can be generated: (i) upgraded shape memory characteristics, e.g. greater shape memory effects that are also less sensitive to degradation, (ii) upgraded structural characteristics, e.g. self-repairing properties resulting in increased resistance to fatigue and buckling of the polymer matrix composite, (iii) combination characteristics, e.g. structural polymer matrix composite with adjustable shape, and (iv) completely new product characteristics, e.g. polymer matrix composites with suitable stiffness and frequency modes. A first prerequisite to the 'design' of these smart materials is that the behaviour of the composing elements is known and predictable. As mentioned above, however, the thermo-mechanical behavior of SMAs is non-linear with hysteresis. In spite of many attempts, the models presented in literature have not yet been very successful in the quantitative description of shape memory behaviour. Another prerequisite is a thorough knowledge of the SMA-matrix interface and its stability during cyclic applications. The curing of the matrix material can influence the behaviour of the embedded element and thus restrain shape memory elements. In conclusion, although smart materials with embedded shape memory elements offer very promising prospects, several topics have to be further investigated before commercial applications can be developed. Great progress can be expected in the next few years.

1.5 Smart Materials and Composites

Smart materials are expected to revolutionize actuation damping systems and biomedical applications and have been identified as one of the most important emergent materials. Davidson [4] gives a definition of the term smart material (also described as *intelligent, sense-able, multifunctional* or *adaptive* materials) as materials that demonstrate their own functions intelligently, depending on sensed environmental changes.

Furthermore, other definitions have been proposed to classify this new technology [4]:

Type I - Passive smart structures (sensors): these have a structurally-integrated optical microsensor system for determining the state of the structure and possibly the environment in which it operates.

Type II - Reactive smart structures (actuators): these have an optical nervous system and an actuator control loop to change some aspects such as the stiffness, shape, position, orientation or velocity of the structure.

Type III - Intelligent structures (real time processors like the human brain): these will be structures capable of adaptive learning.

The smart composites are materials that are technologically advanced and that can combine the mechanical proprieties of composites with the actuation proprieties of smart materials.

They mostly include polymeric matrix with SMA wires embedded inside that are able to react to external impulses. The matrix could be a thermosetting or thermoplastic polymer, and also a reinforced matrix with Kevlar, glass or carbon fibers to improve the mechanical properties.

Smart materials are expected to revolutionize actuation damping systems and biomedical applications and have been identified as one of the most important emergent materials.

There is no universally accepted definition of the term smart material (also described as *intelligent, sense-able, multifunctional or adaptive* materials); however, they can be thought of as materials that demonstrate their own functions intelligently depending on sensed environmental changes.

Shape memory alloys and smart composites with embedded SMA can be defined as type II. The plastically deformed fibers become an integrated part of the composite material structure. When the fibers are heated, generally by means of Joule effect, they are restrained from recovering to their memorized length by the composite and generate a uniformly distributed shear load along

the entire length of the fiber. If the fibers are offset from the neutral axis the structure will deform in a predictable manner. [5].

An alternative method of use is to place the SMA fibers either in or on the structure in such a way that there are no resulting large deformations when actuated, but instead the structure is placed in a residual state of strain, and the modal response of the structure is modified. It has been demonstrated that such techniques can change the effective stiffness, natural frequencies and mode shapes of composite plates [6]

The adhesion between the wires and the selected matrix is extremely important to design smart composites as, by means of the interfacial bond, it is possible to transfer the stress from wire to matrix having the actuation response. Great affords must be done in order to optimize the wire-matrix interface, through mechanical or chemical treatment on the wire surfaces.

1.6 Guidelines to design SMA composites

Shape Memory Alloy (SMA) composites are regarded as promising candidates of the so-called "smart materials".

Investigations over the past decades have demonstrated that shape memory composites have many novel or improved properties such as enhanced high-temperature mechanical properties, shape control, fatigue resistance, vibration damping, acoustic radiation and transmission control, and impact resistance abilities.

However, little has been reported on industrialized shape memory composites, mainly because of their complex behavior that is still not fully understood, and the lack of clear guidelines to optimize the design of shape memory composites.

Looking at the work of Reynaerts and Van Brussel[7] and the work of Zheng, Cui, Schrooten [8], it is possible to find some basic guidelines for designing shape memory composites.[9]

When selecting SMA components, the choice is between NiTi based alloys and copper based alloys.

NiTi based alloys are the best SMA family for smart material actuator applications, mainly because of their excellent mechanical properties. Copper based alloys and ternary alloys are of particular interest because of their relatively small hysteresis.

Finally, NiTi alloys are preferred because their functional properties are far better reproducible: NiTi has higher mechanical strength, allows higher working stress and also shows a higher memory strain; NiTi also has claimed corrosion resistance comparable to stainless steel.

Other important aspects to consider are the cooling system after actuation, transformation hysteresis and how it is affected by the presence of the matrix, as well as the fatigue behavior.

To select the matrix, it has to be considered that the manufacturing process of SMA composites with a polymer matrix involves pre-straining and maintaining the SMA wires while the matrix is cured in the furnace. To make sure the curing cycle will not affect the shape memory effect, it must be performed at temperature lower then As. If the matrix is a thermosetting polymer, the working temperature of the smart composite should be well below the glass transition temperature Tg of the resin matrix to avoid softening of the resin. For an SMA composite, the interface between the SMA wires and the matrix may fail at a temperature far below Tg because of the build up of recovery stresses. Thus, evaluation of the interface degradation upon heating is necessary to define the maximum working temperature of an SMA composite.

Another factor we need to consider is the pre-strain level of the embedded SMA wires which significantly affects the behavior of an SMA composite. It is widely accepted that a higher pre-strain can provide a higher ultimate recovery stress but at the same time a high pre-strain significantly reduces the reliability of the interface. This implies that a compromise is necessary between mechanical properties and reliability of an SMA composite when selecting the pre-strain level of the embedded SMA wires.

The working temperature of a thermosetting resin composite should be well below the glass transition temperature Tg of the resin matrix to avoid softening the resin. For an SMA composite, the interface between the SMA wires and the matrix may fail at a temperature far below Tg because of the building up of recovery stresses. Thus, evaluation of the interface degradation upon heating is necessary to define the maximum working temperature of an SMA composite.

Further development in this field is to design a hybrid smart composite, in which the use of glass fibers in the matrix together with embedded SMAs wires can open up new developments in actuators.

References

[1]   K. Otsuka, C.M Wayman, Shape memory materials Cambridge University Press Cambridge UK 1998.

[2]   K. Otsuka, X. Ren, Physical metallurgy of Ti–Ni-based shape memory alloys, Prog. in Mater. Sci. 50 (2005), 511-678.

[3]   K. Otsuka, X. Ren, martensitic transformations in nonferrous shape memory alloys, Mater. Sci. and Eng. 273-274 (1999), 89-105.

[4]   R. Davidson. Smart composites: where are they going? Materials&Design vol13 No2 April 1992 pp87-91.

[5]   C.A. Rogers, D. K. Berk, K.D. Bennett, Demonstration of a smart material with embedded actuators for active control. *SPIE,* Vol. 986, 1988, pp 90-105

[6]   M.W. Lin and C.A. Rogers, Fundamental design issues related to SMA reinforced composites. SPIE, Vol. 1170, 1989.

[7]   B.D. Reynaerts, H. Van Brussel, Design aspects of shape memory actuators, Mechatronics 8 (1998) 635-636.

[8]   Y.J. Zheng, L.S. Cuia, J. Schrootenb Basic design guidelines for SMA/epoxy smart composites, Materials Science and Engineering A 390 (2005) 139–143.

[9]   Dazhi Yang, Shape memory alloy and smart hybrid composites-advanced materials for the 21stCentury, Materials and Design 21 (2000) 503-505

ARTICLES

ARTICLE 1

USING DSC AND DMTA FOR THE STUDY OF THERMO-MECHANICAL TREATMENTS IMPROVING THE TRANSFORMATIONAL BEHAVIOUR OF TI-RICH NITINOL SHEETS

Mattia Merlin, Martina Scoponi

Department of Engineering, University of Ferrara, Via Saragat, 1 I-44100 Ferrara, Italy. (Mattia Merlin: mattia.merlin@unife.it , Martina Scoponi: martina.scoponi@unife.it)

Abstract

The influence of thermo-mechanical treatments on TiNi shape memory alloys has been studied with Differential Scanning Calorimetry (DSC) and Dynamic Mechanical Thermal Analysis (DMTA). The DSC is a widely used technique to study the transformation temperatures and the behaviour of TiNi alloys. Even though DMTA is a well-known technique, it is not so commonly used with this kind of materials. In this paper both techniques have been applied to TiNi strips subjected to different cycles of annealing, cold rolling and quenching. The aim of the work is to find and characterise the best thermo-mechanical treatment in TiNi thin sheets that controls the transformation temperature and the recovery force during constrained activation. The results of DSC and DMTA have been compared to find a correlation between the two different techniques that may allow the behaviour of a constrained shape memory alloy and the influence of an applied stress on the transformation temperatures to be studied.

Keywords

TiNi shape memory alloys, heat treatments, thermal analysis.

Introduction

Shape memory alloys (SMAs) are known because they have the skill to remember a predetermined shape even after severe deformation. Depending on the temperature and on applied stress, a SMA can be in the austenitic or in the martensitic phase [1].

In TiNi alloys the austenitic phase, known also as the parent phase, is a B2 type ordered structure stable at high temperature, while at low temperature or high stresses the martensitic phase, which has a B19' structure, is preferred [1].

The shape memory effect is due to the reversible martensitic transformation, which takes place when transformation temperatures are reached. Ms and Mf are defined as the temperatures at which the transformation from austenite to martensite starts and finishes, while inverse transformation, from martensite to austenite, takes place between As and Af.

The temperature range depends mainly on the chemical composition, in Ni-rich alloys Ms could decrease to 100 K (increasing the Ni content), while in Ti-rich alloys Ms is almost composition-independent till the maximum content of Ti and its value is around 333 K (Timax= 51at.% for the solubility limit in the TiNi phase diagram) [2].

DSC analysis is a well-known technique in the field of TiNi alloys, and it has been successfully applied in order to determine transformation temperatures [1,2,3,4]. Among SMAs, the most widely studied for their good mechanical and corrosion behaviour are those based on the TiNi binary system. In particular, TiNi alloys show the unique capability of generating large stresses or recovering large strains (over 7%) during the martensitic transformation [1]. If a prestrained SMA is constrained during transformation from martensite to austenite (i.e. embedded in a polymer matrix), the shape memory effect can generate large recovery stresses up to 800 MPa [5].

Thermo-mechanical treatment is fundamental to control transformation temperatures, the shape memory effect and the transformation stress during recovery [5]. The most common thermo-mechanical treatments are ausforming and marforming, in which some defects are introduced into the austenitic and martensitic lattice, respectively [6,7].

Different authors have studied the correlation between the heat treatment of Ni-rich SMAs and their mechanical properties [6,7,8,9,10]. In other works, attention has been mainly focused on the phase transformation of Ti-rich alloys by changing the processing conditions, such as thickness reduction, heat treatment temperature or time and chemical composition [10,11,12,13].

In this paper attention has been focused on a commercial Ti-49.2at.%Ni alloy, in which the Ti content is close to the solubility limit and the Ms above room temperature allows this alloy to be used for smart actuators working at 373 K. The goal is to identify a thermo-mechanical treatment in order to obtain As > 363 K, the maximum recovery force and a fully reversible behaviour during the activation cycle, by means of cold deformation and a specific heat treatment.

The transformation temperatures are determined by two different techniques, that are Differential Scanning Calorimetry (DSC) and Dynamic Mechanical Analysis (DMTA) and the results are compared. The first method is commonly used with this kind of material, while the second is more commonly applied to polymeric materials to investigate their viscoelastic temperature-dependent behaviour.

In the case of shape memory materials, the DMTA could be useful to investigate the behaviour during activation when the material is externally constrained. Through DMTA analysis, it is possible to qualitatively evaluate the recovery force during the constrained activation, by measuring the values of the modulus in the austenitic phase according to the different heat treatments [14].

Experimental procedures

Some rectangular shaped Ti-49.2at.%Ni strips, with a thickness of 0.5 mm and a width of 5 mm, were obtained by electro-erosion. The strips were first annealed at 1073 K for 1 h in a furnace to remove the previous thermo-mechanical treatment, and then the oxide layer on the surface was removed by etching in a HNO3 solution at 30 vol.% for 30 min.

The strips only subjected to the annealing treatment were considered as reference samples in both the DSC and DMTA analyses. Other strips were cold-rolled with a thickness reduction of 20% and 30%, respectively. Within the two sets of samples, with different thickness reduction, the strips were subjected to different heat treatments; after a solubilisation performed at the

assigned temperatures of 673, 773 or 873 K for 30 min, they were then quenched in water at room temperature.

All the strips were cut into specimens with the specified dimensions to be analysed in the DSC and DMTA machines: for the DSC the samples had a weight of 10 mg, for the DMTA the samples had a length of 25 mm, a width of 5 mm and a thickness of 0.4 mm (20% thickness reduction) or 0.35 mm (30% thickness reduction). The samples were named according to the thickness reduction and the heat treatment they were subjected to, as collected in Table 1.

The samples were analysed with a Mettler Toledo DSC to determine the transformation temperatures and the heats without any applied stress, with a heating and cooling rate of 10 K/min. Instead, the DMTA technique was used in order to study the transformation temperatures under applied load and to evaluate the modulus during thermal activation. The DMTA analysis was carried out with a strain amplitude of 0.3% and a frequency of 1 Hz, by using a single cantilever bending configuration. For both the DSC and DMTA analyses the temperature range of 298÷473 K was selected.

Table 2.1: Samples and condition of the thermo-mechanical treatments.

Sample	Treatment condition
R	Annealed at 1073 K
Set 1	
x_20	Annealed and cold-rolled at 20%
20_T673	Annealed and cold-rolled at 20% and quenched at 673 K
20_T773	Annealed and cold-rolled at 20% and quenched at 773 K
20_T873	Annealed and cold-rolled at 20% and quenched at 873 K
Set 2	
x_30	Annealed and cold-rolled at 30%
30_T673	Annealed and cold-rolled at 30% and quenched at 673 K
30_T773	Annealed and cold-rolled at 30% and quenched at 773 K
30_T873	Annealed and cold-rolled at 30% and quenched at 873 K

Results

The transformation temperatures were evaluated by means of the DSC analysis. In Figure 2.1 the thermal behaviour of the reference sample (R) is depicted under controlled heating and cooling conditions. During heating, the endothermic peak is the phase transformation from martensite to austenite, while the exothermic peak is the phase transformation from austenite to martensite during cooling. The latent heats per unit mass associated to the phase transformation were evaluated by the integration of the peaks, while the transformation temperatures were identified as the intersection between the base line and the tangents to the curves at the peaks.
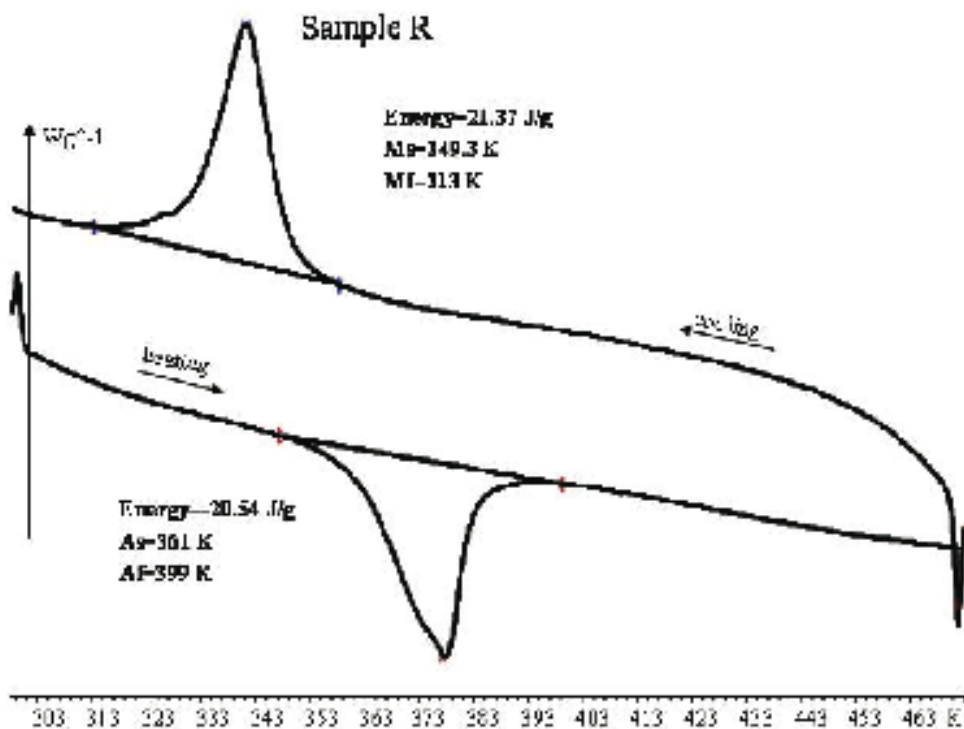
Fig. 2.1: Dsc curve of the Reference sample.

In sample R the latent heats associated to the martensite-austenite direct and inverse phase transformations are quite similar, i.e. the two phases show complete reversibility. The results obtained from the DSC tests of the other samples point out that the higher the treatment temperature the higher the energy associated to the transformation and the temperature As. The

values of the energy and of the transformation temperatures of each sample are reported in Table 2.2. The samples quenched at 773 K have the highest energy associated to the transformation and the maximum reversibility.

Table 2.2: DSC results - temperature and heats of phase transformations.

Sample	M_f [K]	M_s [K]	ΔH [J/g]	A_s [K]	A_f [K]	ΔH [J/g]
R	313	349	21.37	361	399	20.54
20_T673	301	335	6.29	322	367	16.14
30_T673	268	316	6.93	333	368	23.93
20_T773	313	334	28.75	360	379	28.50
30_T773	309	335	23.34	361	387	18.14
20_T873	304	346	27.28	373	413	23.99
30_T873	322	347	27.50	377	401	25.67

The transformation temperatures are more influenced by the quenching temperature than the thickness reduction; the latter mostly affects the heats of transformation and the thermal hysteresis. In Figures 2.2 and 3.2 the transformation temperatures of the samples with different thermo-mechanical histories are shown. The samples quenched at 873 K have the highest As temperatures; the high temperature treatment after cold deformation restores the lattice orientation as in the reference sample.
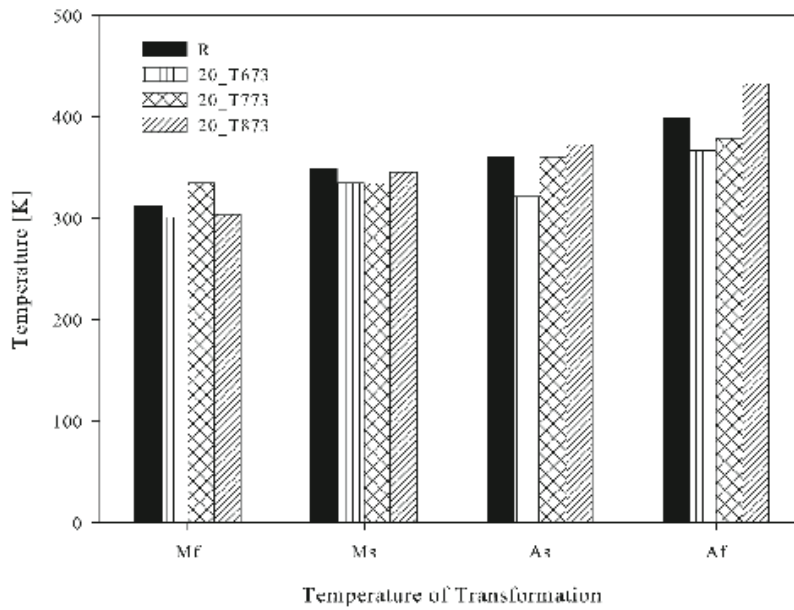
Fig. 2.2: Transformation temperatures of the samples cold rolled at 20% of thickness reduction.
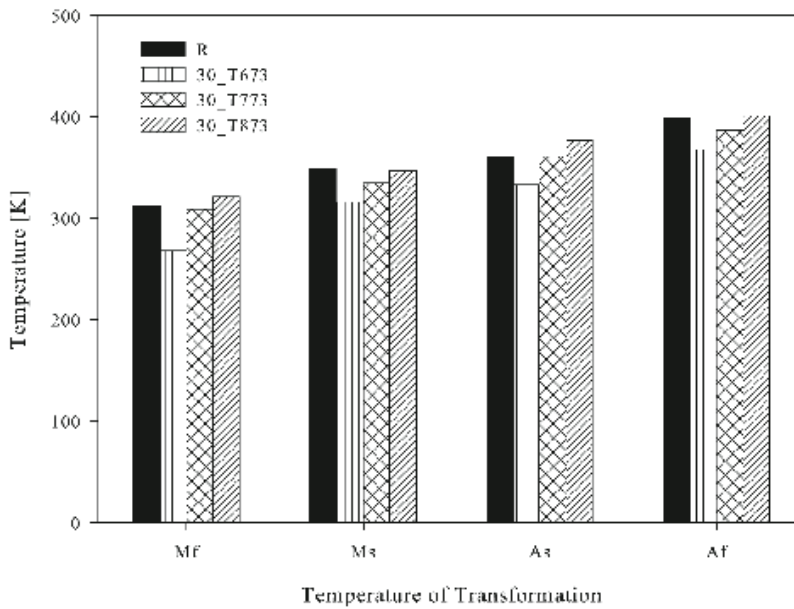

Fig. 2.3: Transformation temperatures of the samples cold rolled at 30% of thickness reduction.

In Figures 2.4 and 2.5 the thermal behaviour of the samples x_20 and x_30, subjected only to cold rolling, are depicted. As shown in previous works, there are two different kinds of martensite microstructures in a shape memory alloy: the self-accomodating martensite (SAM) and the preferentially oriented martensite (POM). The transformation of POM does not show a contribution to the heat flux measured in the DSC test; the heat flux registered by the instrument is produced by the SAM variants [5]. In the samples x_20 and x_30, due to the cold rolling process there is no heat flux associated to the transformation and thus the martensite is totally POM.
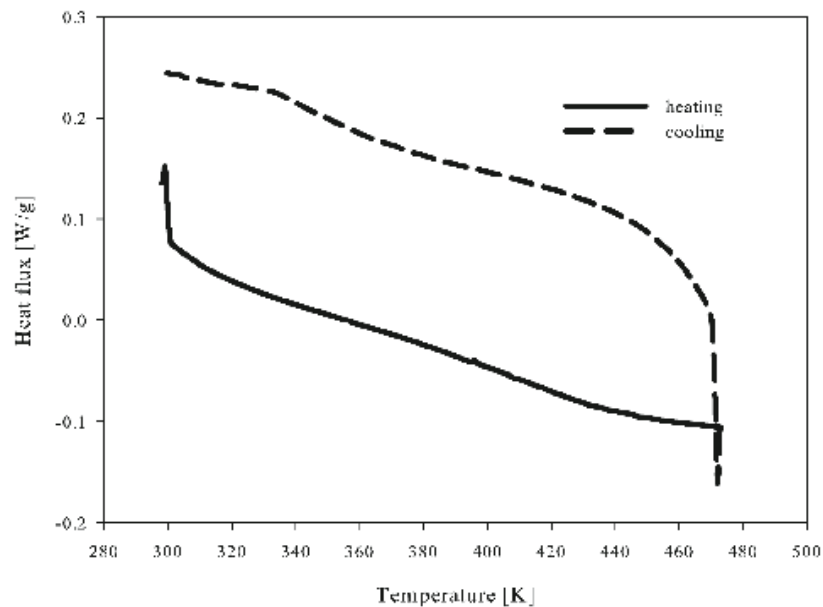
Fig. 2.4: Dsc curve of sample x_20 in which there is no endothermic or exothermic peak of transformation.
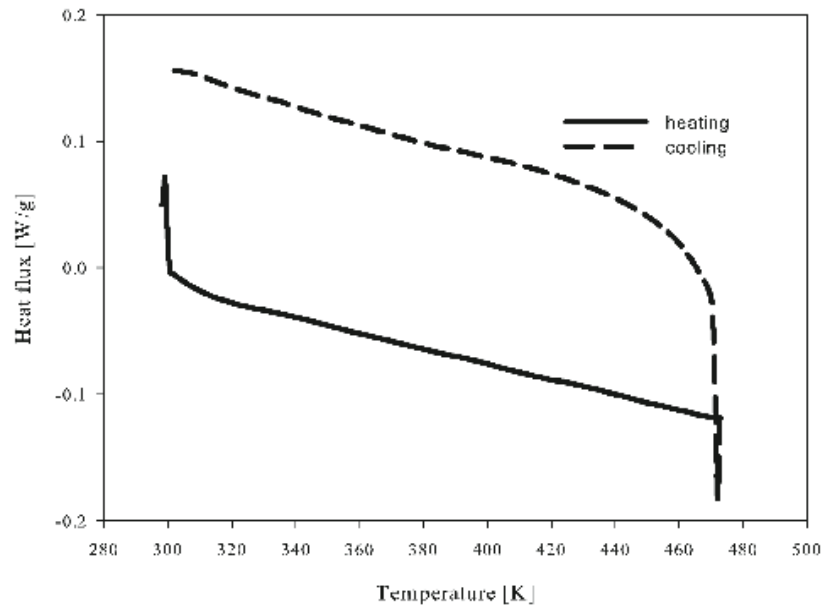
Fig. 2.5: Dsc curve of the sample x_30 in which there is no endothermic or exothermic peak of transformation.

The sample 30_T673 shows a two-step transformation, as can be seen in Figure 6; in a previous paper, this behaviour was attributed to the presence of the R-phase [4]. The R-phase is a rhombohedral phase that may appear in the presence of specific alloying elements or severe deformation and ageing of the martensite. The R-phase has a detrimental effect on the recovery force generated during the constrained recovering of the shape. Figure 2.6 shows that during the cooling of sample 30_T673, two exothermic peaks appear: the peak at higher temperature is the transformation from austenite to R-phase, while the other peak is related to transformation from R-phase to martensite [1]. In the other samples, the R-phase does not occur because the cold deformation is less drastic or because the quenching temperature is high enough to reduce the lattice distortion caused by the deformation.
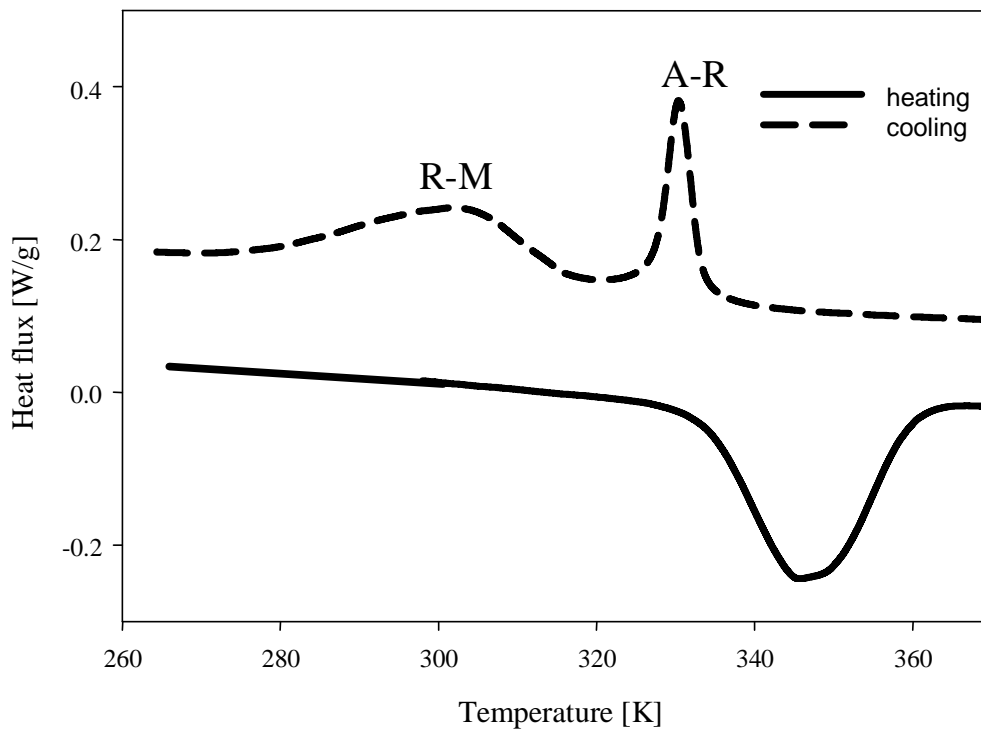
Fig. 2.6: Dsc curve of the sample 30_T673 in which appears the R-phase during the cooling of the sample.

The thermo-mechanical behaviour of the alloy was also studied by using the DMTA technique. DMTA is mostly applied in polymeric materials where this particular technique allows the transition from elastic to viscoelastic behaviour to be observed, with increasing temperature. In SMA materials the DMTA could be useful to measure a modulus (different from the elastic modulus), which can give us information about the response and the strength of the samples in a constrained-activation. The modulus measured by the DMTA at room temperature and the modulus measured at a temperature higher than As are useful parameters in order to choose the best thermo-mechanical treatment with the highest recovery force.
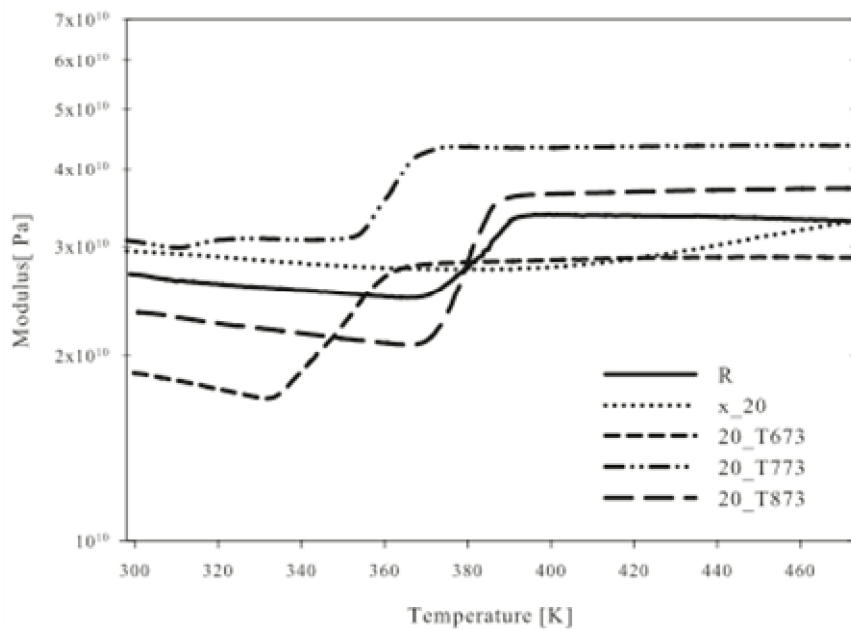
Fig. 2.7: Development of the modulus during the DMTA test of samples cold rolled at 20% of thickness reduction.
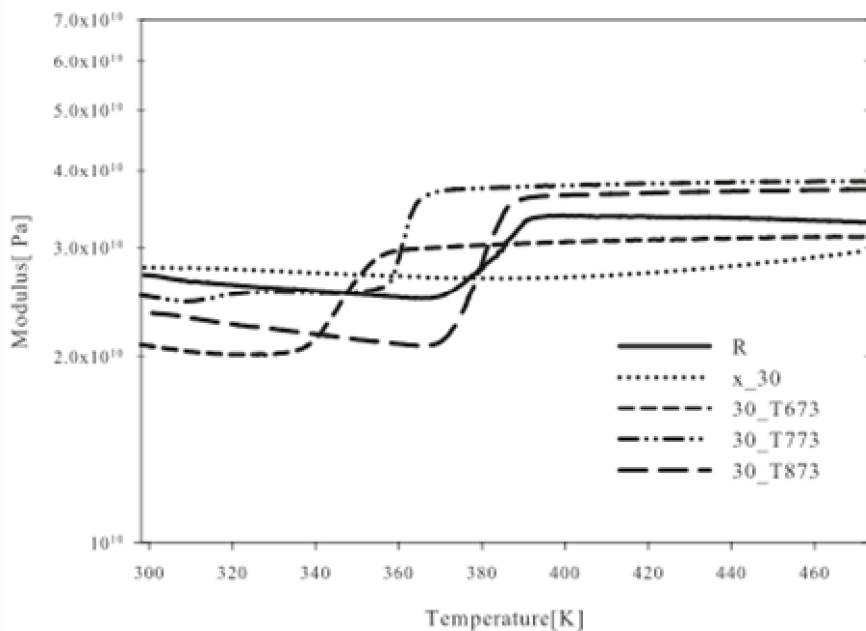
Fig. 2.8: Development of the modulus during the DMTA test of samples cold rolled at 30% of thickness reduction.

In Figures 2.7 and 2.8, the DMTA curves are reported; as in the DSC curves, the samples subjected only to cold rolling do not show any transformation. The quenching temperature influences the modulus more than the thickness reduction and, as can also be seen in Table 3, samples quenched at the same temperature show a similar behavior during the DMTA test either for range of transformation, either for the values of flexural modulus. In Table 2.3 the transformation temperatures extrapolated from the DMTA curves are reported. In agreement with the DSC results the samples 20_T873 and 30_T873 have a behavior similar to the reference sample.

**Table 2.3: DMTA results – temperatures of the austenitic transformation.**

Sample	A_s [K]	A_f [K]	E_m^* [GPa]	E_a^* [GPa]
R	366	371	26.8	33.5
x_20	-	-	29.4	29.4
x_30	-	-	27.8	27.8
20_T673	327	362	18.5	28.5
30_T673	328	356	22.5	28.5
20_T773	359	373	30.3	43.3
30_T773	354	374	25.0	37.5
20_T873	346	384	23.3	36.3
30_T873	368	387	23.3	36.3

* The martensitic modulus was taken at 293 K, while the austenitic modulus was taken at As according to the transformation temperatures of each sample.

As the quenching temperature is increased, the transformation temperatures (especially As) increase as can be observed also in the DSC test. The transformation temperatures calculated with the DSC and the DMTA technique are very similar for the sample in which the prevalent martensite variant is SAM, as can be seen in Figure 2.9. Otherwise in the samples 20_T673 and 30_T673 subjected to a stronger cold deformation have very different As temperatures.
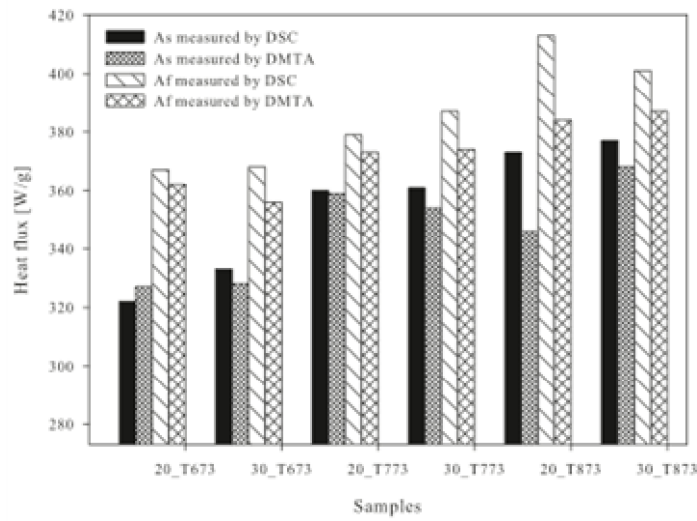
Fig. 2.9: Comparison between transformation temperatures measured by DSC and DMTA.
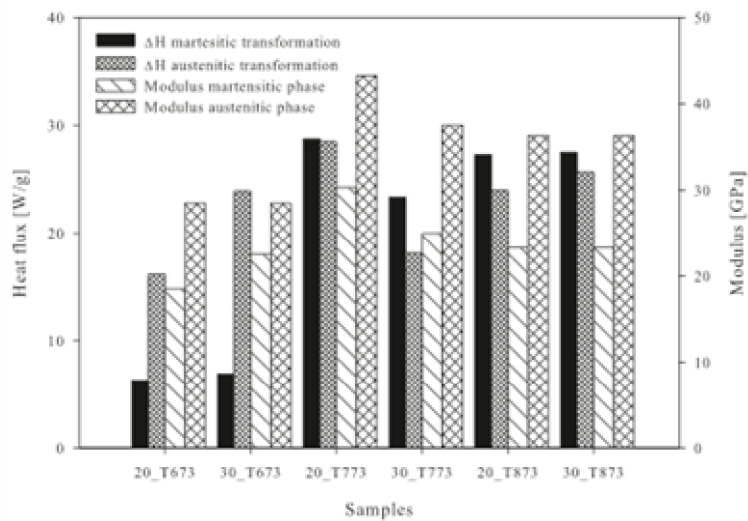
Fig. 2.10: Comparison between DSC and DMTA data.

The samples with the higher modulus in the austenitic phase are those quenched at 773 K and the austenitic modulus is correlated with the recovery force during activation. Moreover, a direct correlation between the transformation heats calculated by DSC and the modulus measured by DMTA can be found, as depicted in Figure 2.10. As observed in the figure the sample 20_T773,

for which the phase transformation latent heats are similar on heating and on cooling, shows the highest austenitic and martensitic moduli.

Conclusion

The selection of the best thermo-mechanical cycle in NiTi shape memory alloys is very important for the development of mechanical actuators. DSC and DMTA tests have been carried out on Ti-rich Nitinol strips subjected to different thermo-mechanical treatments. Even though DSC is traditionally used to characterise the transformation temperatures of shape memory alloys, it has been shown that DMTA can also contribute to the study of this kind of materials, in particular when they are designed to work as actuators. A correlation between both DSC and DMTA results exists in the examined samples. In fact, the samples with the highest transformation energy in the DSC analysis also have the highest modulus measured with the DMTA.

In this work information has been obtained for the thermo-mechanical training needed to achieve the best compromise between the transformation temperatures, the recovery force and the phenomena reversibility.

Based on the obtained results regarding the influence of cold deformation and quenching temperature on the shape memory behaviour (see Figure 10), the following conclusions can be drawn:

- As predicted, the samples cold-rolled with a 20% and 30% thickness reduction and without any further heat treatment show no transformation in the DSC and DMTA curves, because the martensite is preferentially orientated (POM).

- The samples quenched at 873 K have the highest As values and their behaviour in the DSC and the DMTA test is similar to the reference sample.

- The samples with thickness reduction of 20% or 30% and quenched at 773 K show the best improvement in the modulus and in the recovery force.

- The samples quenched at 673 K have a large thermal hysteresis and show the lowest transformation temperatures. Furthermore, there is also the appearance of the R-phase in the sample cold-worked at 30% of thickness reduction. The presence of the R-phase decreases the shape memory effect and also decreases the recovery force during

activation: in fact, in the sample the DMTA test enlightens the poor mechanical behaviour in both the martensitic and the austenitic phases.

ACKNOWLEDGEMENTS

REFERENCES

[1]   K. Otsuka, C.M. Wayman, Shape Memory Alloys. Cambridge University Press 1998; pp 1-5; 49-71; 149-158.

[2]   K. Otsuka, X. Ren, Physical metallurgy of Ti–Ni-based shape memory alloys, Prog. in Mater. Sci. 50 (2005), 511-678.

[3]   K. Otsuka, X. Ren, martensitic transformations in nonferrous shape memory alloys, Mater. Sci. and Eng. 273-274 (1999), 89-105.

[4]   J. Uchil, F.M. Braz Fernandes, K.K. Mahesh, X-ray diffraction study of the phase transformations in NiTi shape memory alloy, Mater. Charact. 58 (2007), 243-248.

[5]   K.A. Tsoi, R. Stalmans , J. Schrooten, Transformational behaviour of constrained shape memory alloys, Acta Mater. 50 (2002), 3535-3544.

[6]   D. Wurzel, Marforming and tempering of binary Ni–Ti alloys including precipitation effects, Mater. Sci. and Eng. A273-275 (1999), 634-638.

[7]   P. Filtp, K. Mazanec, Influence of work hardening and heat treatment on the substructure and deformation behaviour of TiNi shape memory alloys, Scr. Metall. et Materi. 32(9) (1995), 1375-1380.

[8]   Z.G. Wang, X.T. Zu, X.D. Feng, S. Zhu, J.M. Zhou, L.M. Wang, Annealing-induced evolution of transformation characteristics in TiNi shape memory alloys, Phys. B 353 (2004), 9-14.

[9]   D.A. Miller, D.C. Lagoudas, Influence of cold work and heat treatment on the shape memory effect and plastic strain development of NiTi, Mater. Sci. and Eng. A308 (2001), 161-175.

[10]   T.Kurita, H. Matsumoto, H. Abe, Phase transformation behavior of Ti-rich NiTi alloy by a calorimetric method, J. Mater. Sci. 39 (2004), 4391-4392.

[11]   I. Karaman, H.E. Karaca, H.J. Majer, Z.P. Luo, The Effect of Severe Marforming on Shape Memory Characteristics of a Ti-Rich NiTi Alloy Processed Using Equal Channel Angular Extrusion, Metall. And Mater. Trans. 34A (2003), 2527.

[12]   A.S. Paula, K.K. Mahesha, C.M.L. dos Santos, F.M. Braz Fernandes, C.S. da Costa Viana, Thermomechanical behavior of Ti-rich NiTi shape memory alloys, Mater. Sci. and Eng. A481-482 (2008), 146-150.

[13]   A.S. Paula, J.P.H.G. Canejo, R.M.S. Martins, F.M. Braz Fernandes, Effect of thermal cycling on the transformation temperature ranges of a Ni–Ti shape memory alloy, Mater. Sci. and Eng. A37 (2004), 92-96.

[14]   R. Artiaga, A. Garcia, L. Garcia,A. Varela, J.L. Mier, S. Naya, M. Grana, DMTA Study of a Nickel-Titanium wire, J. Therm. Anal. and Calorim. 70 (2002), 199-207.

ARTICLE 2

ON THE IMPROVED ADHESION OF NITI WIRES EMBEDDED IN POLYESTER AND VINYLESTER RESINS

Mattia Merlin, Martina Scoponi, Chiara Soffritti

Department of Engineering, University of Ferrara, Via Saragat, 1 I-44100 Ferrara, Italy. (Mattia Merlin: mattia.merlin@unife.it , Martina Scoponi: martina.scoponi@unife.it, Chiara Soffritti: chiara.soffritti@unife.it)

Preprint version.

Abstract

Shape memory alloys (SMAs) are successfully used to realise smart composites in which active elements, in the form of wires or thin strips, are embedded in a polymer matrix. The advantage of the use of these kind of composites is related to the ability of SMAs to generate a macroscopic deformation of whole structures, replacing expensive and cumbersome mechanical systems. The transfer of stresses and strains during thermal activation of the SMA elements depends on the integrity of the SMA wire/polymer interface.

This paper discusses the effect of different surface treatments on shape memory alloy wires embedded in two polyester and vinyelster polymer matrices. In particular, two types of chemical etching and a chemical bonding by a silane coupling agent are performed on the wires' surface in order to improve the adhesion with the surrounding matrix. Pull-out tests are carried out on samples obtained using a specifically designed teflon mould. The results prove that the wires functionalised with a silane agent embedded in the polyester resin show the maximum pull-out forces and the highest interface strength. The scanning electron microscope observations of the

wires' surfaces and the analysis performed with energy dispersive spectroscopy microprobe confirm the pull-out results.

1 Introduction

Shape memory alloys (SMAs) are characterised by the presence of two material phases, the austenite stable at high temperature and the martensite stable at low temperature, and the presence of a thermoelastic martensitic transformation. These alloys are able to show either the shape memory effect or the superelastic behaviour, according to the temperature range and the applied load.

The shape memory effect is the ability of the alloy to recover a mechanically-induced strain when heated over a critical temperature. In particular, for such alloy is fundamental the knowledge of the four transformation temperature: As and Af are the initial and final temperatures of the direct martensitic transformation from austenite to martensite on cooling, while Ms and Mf are the initial and the final temperatures of the inverse martensitic transformation from martensite to austenite on heating [1].

The peculiar functional properties of SMAs has been widely used for the making of actuators, sensors, damping systems and in biomedical applications [2,3]. The ability of these materials to generate high recovery stresses when thermally activated has been recently utilised for the realisation of functional structures or composite, in which SMA elements are indirectly or directly embedded in a polymer matrix, respectively [4-6]. According to the specific application, the choice of the suitable matrix and of the chemical composition of the shape memory alloy is of great importance [7-9].Functional composites, also called smart composites, take advantage of the adhesion between the active elements, in form of SMA wires or thin strips, and the matrix. Many authors studied the transformational behaviour of NiTi wires pre-strained in the martensitic phase (at T<Mf) and embedded in a polymer matrix. The mechanical properties of smart composites depend strongly upon the efficiency of stresses and deformations transfer at the interface between the wires and the surrounding matrix [11-14]. This way, the adhesion quality must be improved in order to avoid the degradation or the premature failure of the actuation response. Many works highlighted that an improvement of the interface adhesion can be achieved by mechanical abrasion [15,16] and chemical passivation by acid solutions [16-19] of

SMA wires' surfaces. Both these methods increase the superficial roughness of the active elements. The chemical etching produces oxide layers leading to a reduction of the alloy volume that displays the shape memory effect. Moreover, debonding could occur at the interface between the oxide layers and the polymer matrix [13]. In [3, 20-22] has been reported the possibility to functionalise the surface of NiTi wires by using silane coupling agents; in particular, pull-out tests have been performed to quantify the improvement of the interface adhesion.

Several test methods, such as push-out [26], pull-out and fragmentation [29] tests have been developed to characterise the wire-matrix interface [22].

The goal of the present paper is to investigate the performance of different surface treatments carried out on NiTi shape memory wires embedded in two polymer matrices in order to improve the interface adhesion. In particular, chemical etching by acid solutions and chemical bonding by a silane coupling agent have been evaluated. The matrices have been chosen among thermosetting resins: polyester and vinylester resins. To complete the polymerisation and to give the suitable mechanical properties, these resins have been cured at a temperature lower than As, the initial temperature for the indirect martensitic transformation. Specific pull-out samples have been realised and tested in order to compare the quality of the different surface treatments according to the polymer matrices. Moreover, the roughness and the morphology of the wires' surfaces have been studied by means of scanning electron microscope with energy dispersive spectroscopy microprobe.

2 Materials and methods

2.2 Materials

A commercially available Ti-50.7at% NiTi alloy has been supplied in the form of thin wires with a diameter of 0.5 mm. The wires have been straight annealed at 800 °C for 1 h in a furnace with an uncontrolled atmosphere and then cooled in air in order to remove the previous thermo-mechanical treatment.

The transformation temperatures (TTRs) and the latent heats per unit mass of the alloy have been evaluated by the Differential Scanning Calorimetry (DSC) technique. The DSC sample has been

heated and cooled at a constant rate of 10 °C/min in the range of the martensite-austenite phase changes; the thermogram is depicted in Figure 3.1 and the main results are collected in Table 3.1.
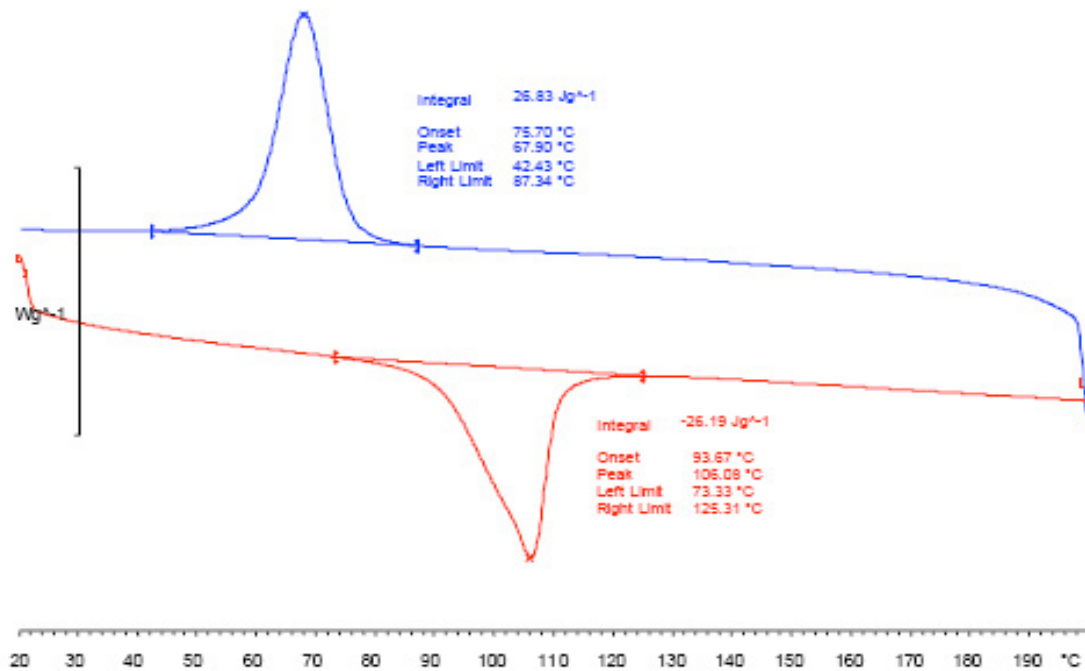

Figure 3.1: DSC thermogram of the annealed NiTi wire.

Table 3.1: Transformation temperatures and latent heats per unit mass of the NiTi wire after annealing.

Mf (°C)	Ms (°C)	As (°C)	Af (°C)	ΔH_M (J/g)	ΔH_A (J/g)
60.00	75.70	93.67	112.00	26.83	26.19

The wires have been subjected to three different surface treatments, as explained in section 2.2, and then embedded in polymeric matrices. In particular, the two thermosetting PolyEster (PE) with a 30%-Styrene content and Vynilester (VE) resins, supplied by Polynt S.p.A., have been considered. The resins needs to be cured to complete the polymerisation and to give the suitable mechanical properties. The NiTi wires must be embedded in the resins before the curing heat

treatment. In order to avoid the phase transformation of the NiTi alloy, a cure temperature lower than the As temperature should be chosen. Accordingly, samples in PE and VE resins have been cured at 90 °C for 2 h and the main physical and mechanical properties of the post-cured resins have been evaluated. The DSC measurements performed on the post-cured resins allowed to determine their glass transition temperatures (Tg). In Figure 3.2 is reported the portion of the thermogram relative to the heating phase for both resins and the Tg values are collected in Table 3.2.
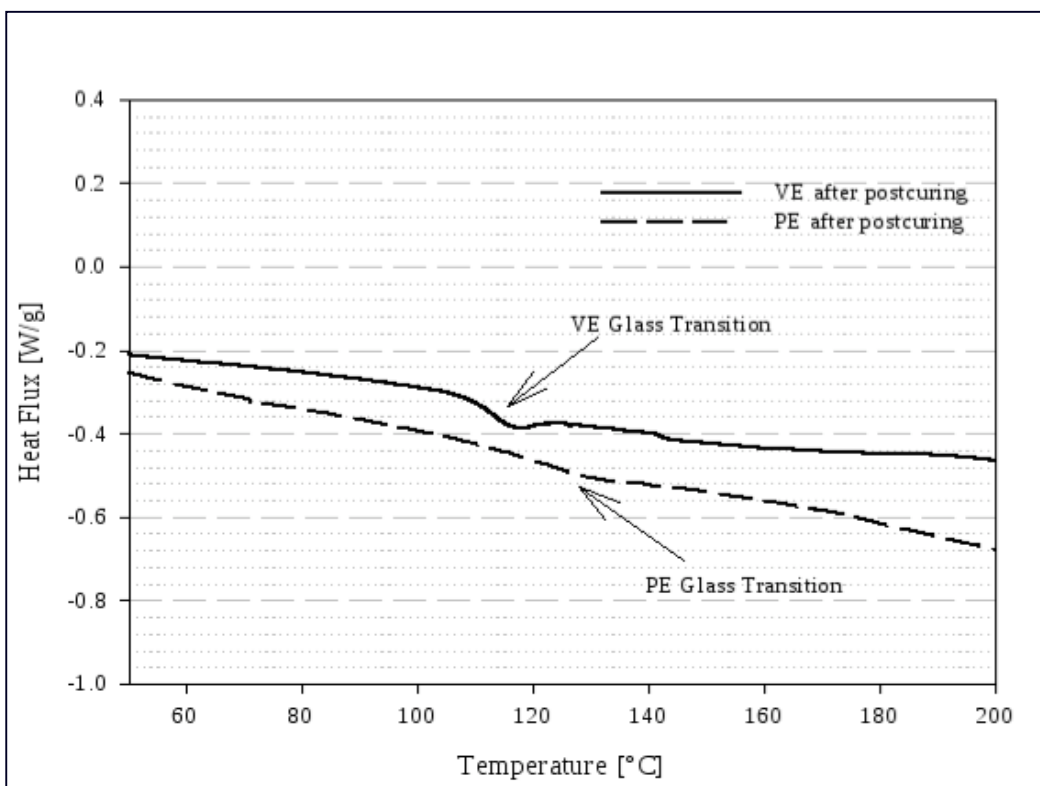
Figure 3.2: DSC thermogram of the post-cured resins.

Table 3.2: Onset glass transition temperatures of the post-cured resins.

Resin	Tg (°C)
PE	110.00
VE	108.00

Three-points flexural tests have been carried out on a Zwick testing machine, according to UNI EN ISO 178:2004. The specimens of both kinds of resins have been milled with dimensions of 80 x 10 x 4 mm from plates polymerised between two glass walls and subsequently post-cured. Five samples of each resin have been tested. The support span was 60 mm, while the cross-head speed was 1 mm/min.

The flexural moduli, maximum stresses and the maximum deformation at break have been determined and the results are depicted in the diagram of Figure 3.3.
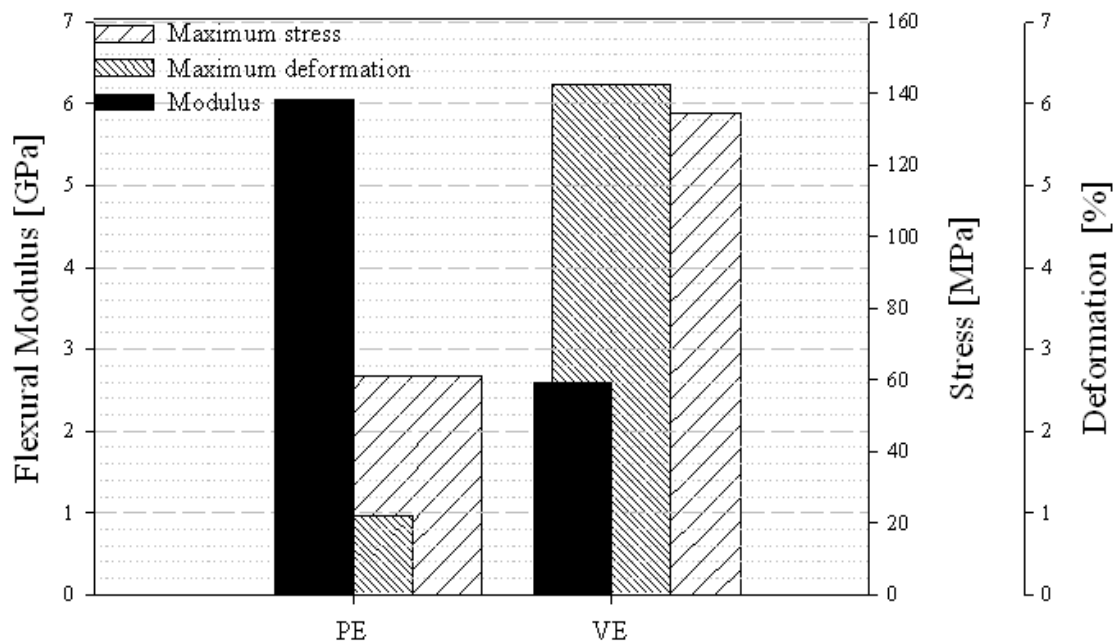
Figure 3.3: Flexural properties of the post-cured resins.

2.2 Surface treatments

Different surface treatments have been performed on the annealed NiTi wires without removing the external oxide layer. First treatment, called A, corresponds to a chemical etching in a 40%HNO3 solution for 30 min. Second treatment, called AB, is a chemical etching in a 5%HNO3 + 15%HF solution for 20 s. Third treatment, called S, is an immersion in a polymetilsilossane coupling agent for 2 h. This three surface treatment have been compared with the wire, called NT, annealed and subsequently cleaned in the methanol solution. In Table 3.3 are summarised the different analysed surface conditions.

Table 3.3: Description of the analysed surface treatments.

| Surface treatment	Description
NT	No surface treatment
A	Chemical etching in a 40%HNO3 solution for 30 min
AB	Chemical etching in a 5%HNO3 + 15%HF solution for 20 s
S	Immersion in a polymetilsilossane coupling agent for 2 h

2.3 Pull-out tests

Pull-out tests have been carried out in order to evaluate the interface strength between the the two polymer matrices and the NiTi wires in the different surface conditions described in section 2.2. The dimensions of the pull-out samples are depicted in Figure 3.4a; in particular, for each sample the wire has been embedded in a 20 mm height cylindrical specimen with a diameter of 10 mm. A specific cylindrical Teflon mould, which consists of three parts as can be noted in Figure 3.4b, has been designed in order to realise the pull-out samples. A polymeric wax has been applied on the internal walls of the mould to prevent the sticking of the resin during the polymerisation and to allow the extraction of the sample.

Three samples for each combination of resin and surface treatment have been realised in order to have a good statistical distribution of the experimental results. All the samples, before the pull-

out test, have been heated in a furnace at 90°C for 2 h in order to complete the polymerisation and to cure the polymer matrices.

The pull-out tests have been carried out by means of a INSTRON 4467 tensile machine with a speed rate of 1 mm/min at room temperature.

After the tests the morphology of the wires' surface has been observed and analysed by a CAMBRIDGE STEREOSCAN S-360 scanning electron microscope (SEM) and by a INCA ENERGY 300 energy dispersive X-ray spectroscopy (EDS).
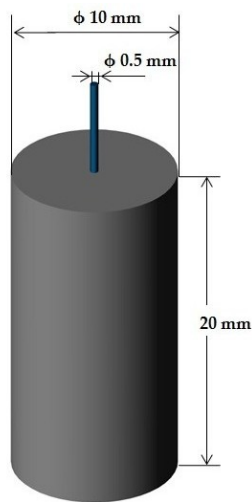
(a)
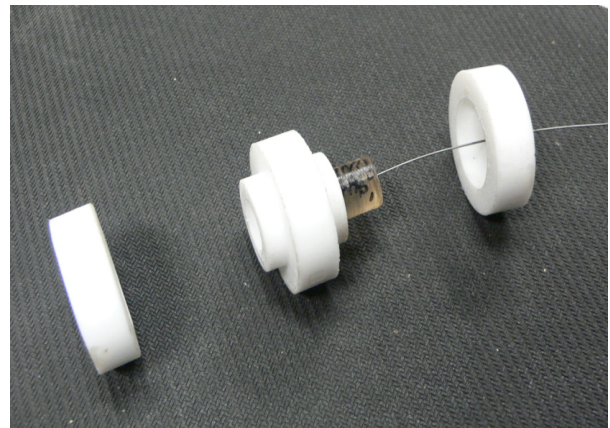
(b)

Figure 3.4: (a) Schematic view of the polymeric cylinder with an embedded pre-strained SMA wire, (b) designed teflon mould and pull-out sample.

3 Results and discussion

In general a typical pull-out curve can be divided in two regions. The first one is characterised by a pre-fracture straining of the interface, in which the applied load increases due to the deformation of the free length of the wire. The force increases until the interface fracture occurs, causing the slip of the wire inside the composite. In some cases, the debonding generates a suddenly drop of the force near to zero, while in others the post-fracture region begins. In this

second region the force can settle down into a lower fairly constant level or can rapidly oscillate around a mean value due to a stick-slip behaviour till the wire completely pulls out [15]. Many theoretical studies [26,27] show that the NiTi-composite interface fails with a typical brittle process and that the interfacial bonding can be evaluated following two different criteria. The first one is based on the assumption that debonding occurs when the shear stress at the interface exceeds the interfacial shear resistance. The second one suggests that the crack initiates at the point of wire entry due to an accumulation of strain; then the crack propagates till the completely debonding of the interface, according to a brittle fracture propagation theory.

In figure 3.5 are depicted the results obtained from the pull-out tests performed on the samples, in which the NiTi wires in different surface treatments are embedded in the two PE and VE resins. In particular, in figure 3.5a are collected the curves related to the pull-out samples realised with PE resin and in the NT, A and AB wire surface conditions. Figure 5b shows the results of the pull-out tests of samples realised with VE resin and in the NT, A and AB wire surface conditions. The pull-out curves of samples in PE and VE resin with wires functionalised by the silane coupling agent are compared in figure 5c.

As can be seen, all curves present a small plateau of 0.2-0.3 mm in correspondence of a ≈15-20 N applied force. This plateau can be compared with the one observed in figure 6, which reports the tensile test for the same free NiTi wire after annealing at 800 °C for 1 h. Therefore, in this initial region of the pull-out test the curve reproduces only the stress-strain behaviour of the free length wire.

In figure 5a can be observed that the debonding suddenly occurs after less than 1 mm of displacement with a load lower than the level necessary to produce the detwinning of the martensitic phase: the VE resin with embedded a no surface-treated wire also shows the same behaviour (figure 3.5b). In contrary, after the small initial plateau in VE_A and VE_AB samples the load further increases and reaches a level sufficient to induce martensitic twin rearrangement. This is in good agreement with the load-displacement curve of the free wire in figure 3.6. In the case of the VE_AB sample the load in which the interface failure occurs is greater than the load in which the phase transformation takes place. According to the model reported in [27], the load increase with a decreasing slope as it approaches the pull-out force is sign of frictional shear force acting on the already bonded fiber. This is in agreement with a brittle fracture propagation theory. Analysing the curves of figure 3.5b, but also of figure 3.5c, another alternative

consideration can be made. As can be noted, the rise of the load after the detwinning plateau begins at a level of displacement lower than the onset of the elastic deformation of the detwinned martensite for the free wire. This behaviour could be justified considering that, after the detwinning of the free length of the wire, the detwinning of the embedded length is partially constrained by the polymer matrix. In the case of VE_A sample the interface failure occurs before the beginning of the martensitic reorientation of the embedded length of the wire: the adhesion is not strong enough to support the increase of the load.

The pull-out curves for the samples with wires functionalised by the silane coupling agent show that the rise of the load after the martensitic plateau is greater than the VE_AB sample. This result, compared with the other specimens, indicates better wetting and chemical adhesion obtained by means of the silane coupling agent.
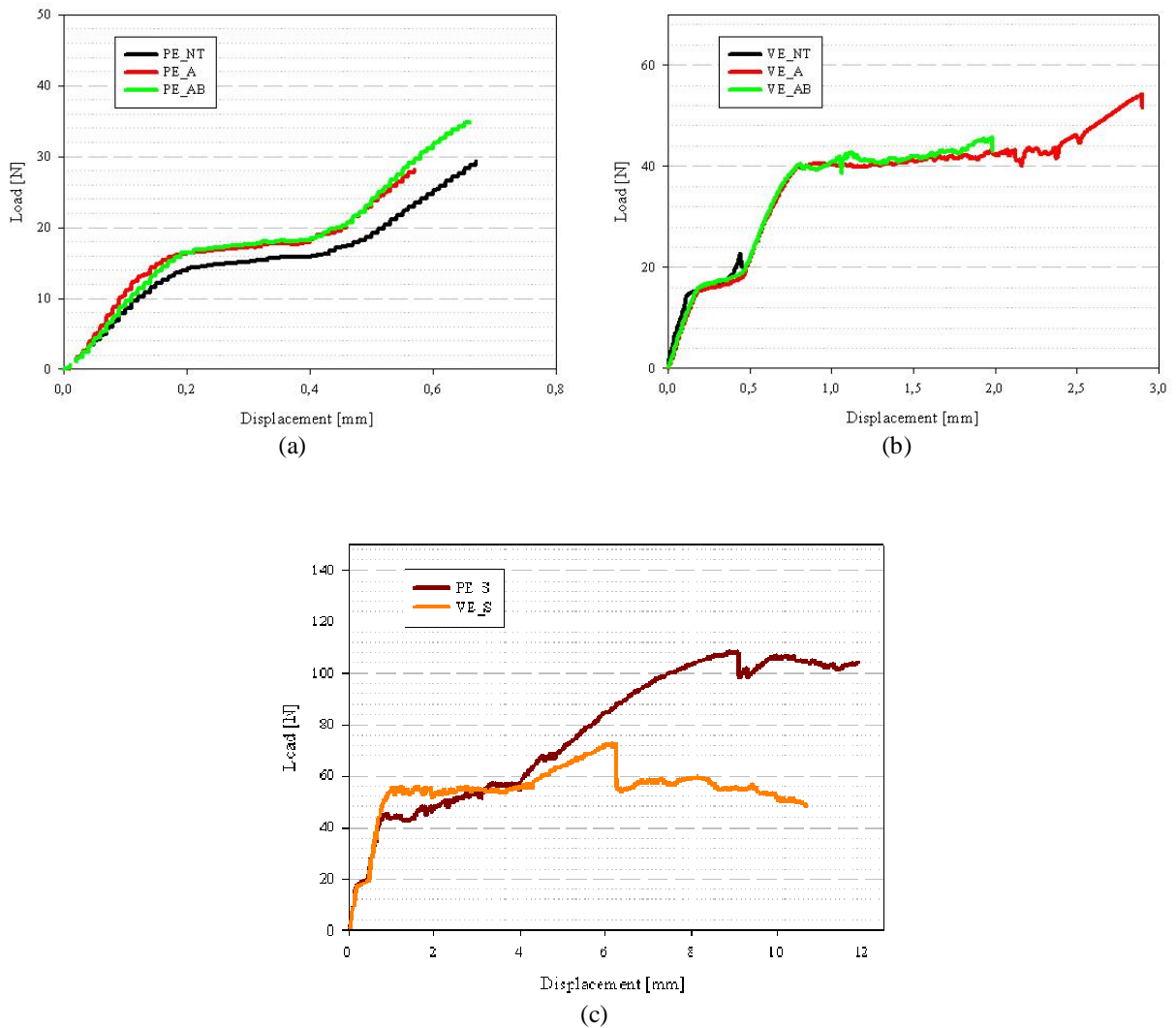
Figure 3.5: Pull-out curves for (a) PE_NT, PE_A and PE_AB samples, (b) VE_NT, VE_A and VE_AB samples, (c) PE_S and VE_S samples.

While in all the other samples the force drops near to zero after the failure of the interface, in PE_S and VE_S samples the force suddenly drops and settles down into a lower value. The wire starts to slip inside the composite and the applied load is now related to the friction acting at the wire-matrix interface. In particular, for the PE_S sample this value is close to the pull-out force, while for the VE_S sample the actual load level is similar to the detwinning plateau load. The PE_S sample shows the best adhesion as manifested by the highest pull-out force.
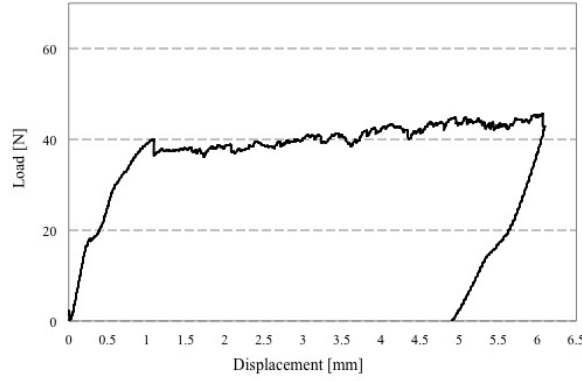
Figure 3.6: Load-displacement curve for the NiTi wire after the annealing treatment.

To better understand the pull out curves the Zandarov Pisanova [29] model has been adopted as a general theory to evaluate the stresses distribution along the embedded wire. The Zandarov-Pisanova model is originally applied for glass fiber embedded in a polymeric matrix, we made the assumption that the Ni-Ti wires behave as a glass fiber because they don't undergo to a phase transformation during the pull-out.

The model allowed us to evaluate the force to produce debonding on the whole wire length Fd and follow the adhesive bond strength τ along the length of the embedded wire with a non uniform distribution of stress hypothesis:

$$\tau(x) = \cosh(\beta x)\left[\frac{F_d \beta}{\pi d}\coth(\beta l_e) + K\tanh(\beta l_e/2)\right] - \sinh(\beta x)\left[\frac{F_d \beta}{\pi d} + K\right] \tag{3.1}$$

With

$$\beta^2 = \frac{8G_m}{E_f d^2 \ln(2R_m/d)}; \qquad K = \frac{E_f SB\beta}{\pi d}; \qquad B = (a_2 - a_1)\Delta T. \tag{3.2}$$

where

G_m = matrix shear modulus;

E_f = wire modulus;

d = wire diameter;

R_m = matrix radius;

S = $\pi d^2/4$ = wire transversal surface area;

α_1= wire thermal expansion coefficient;

α_2= matrix thermal expansion coefficient;

$\Delta T = T-T_r$ where T = pull-out test temperature; T_r = reference temperature.

According to the model the main part of the initial force according the model is spent to overcome the cohesive force in the meniscus zone which forms at the point near the wire entrance in the matrix.

In figure 3.7 is shown the evaluated t(x) trend along the embedded wire length in the PE matrix. The stress is higher at the further extremity of the wire, $\tau_{max} = \tau(x=0)$ and only the first 4-5 millimeters of wire are subjected to the interface shear stress due to friction in the meniscus zone.
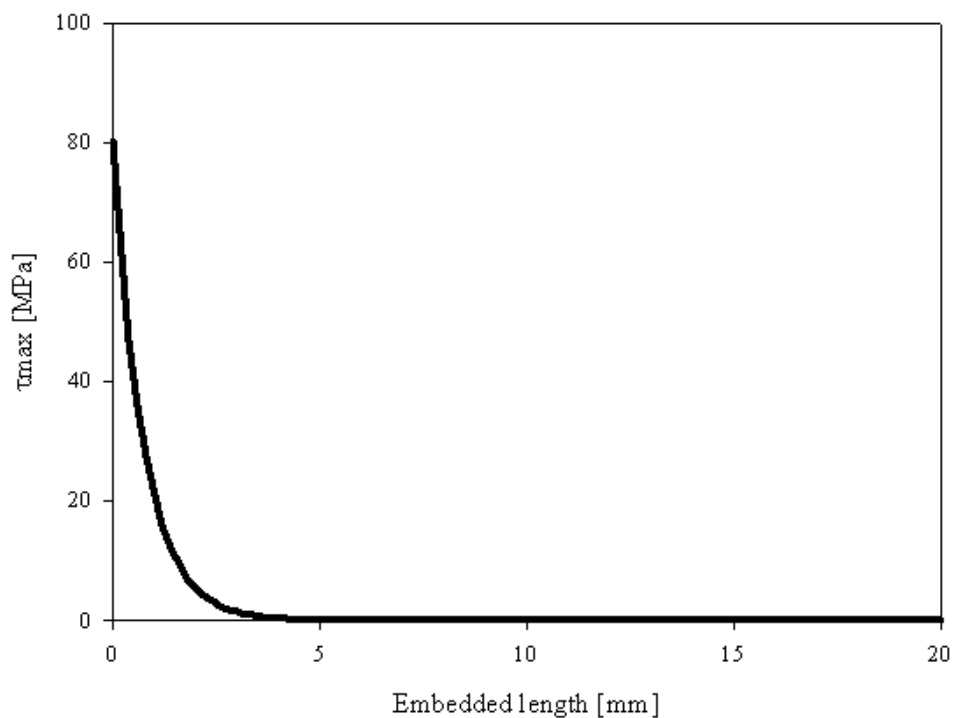
Figure 3.7: Interfacial stress trend during the pull-out test.

In figure 3.8 is shown the confrontation between the different treated wires of the interfacial stress, for this purpose the mean value has been calculated.
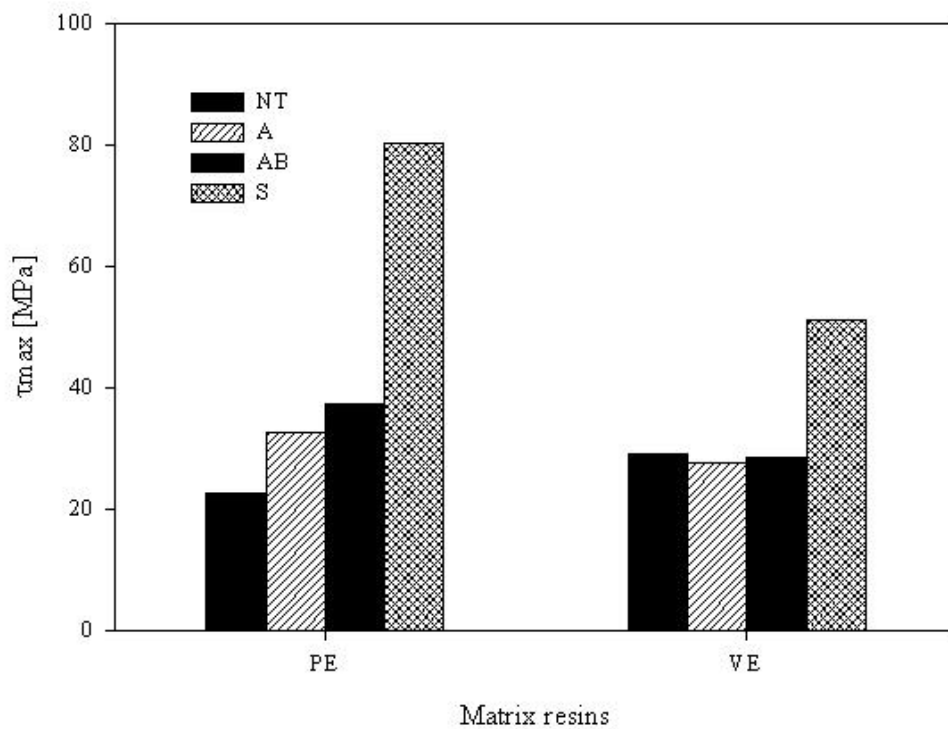
Figure 3.8: Maximum pull-out interfacial stress.

The τ_{max} trend depend only slightly from the matrix, but its value is higher when the wires are treated with silane and decreases with the AB, A and NT following this order.

In this case the PE matrix is the one in which the interfacial stresses are higher and the adhesion bonding is stronger and this is in agreement with the pull out curves in figure 3.5.

The figures 3.9a-d show the surfaces of the treated wires NT, A, AB and S after the pull-out test.

In the picture 3.9a is visible only the oxide layers on the wire surface, while the wires chemically etched show a rough surface especially the wire treated with AB the more aggressive treatment.

On the surface of the silane treated wire instead the darker zone is where the silane had formed the chemical bond with the oxide layer and it was confirmed also by the chemical analysis made with the microscope. The white lines are due to the pull-out test in which the silane coating was

broken and one part remained on the wire while the other one remained on the matrix; this behavior explain the high resistance in the pull-out test. [30-31].

(a)

(b)

(c)

(d)
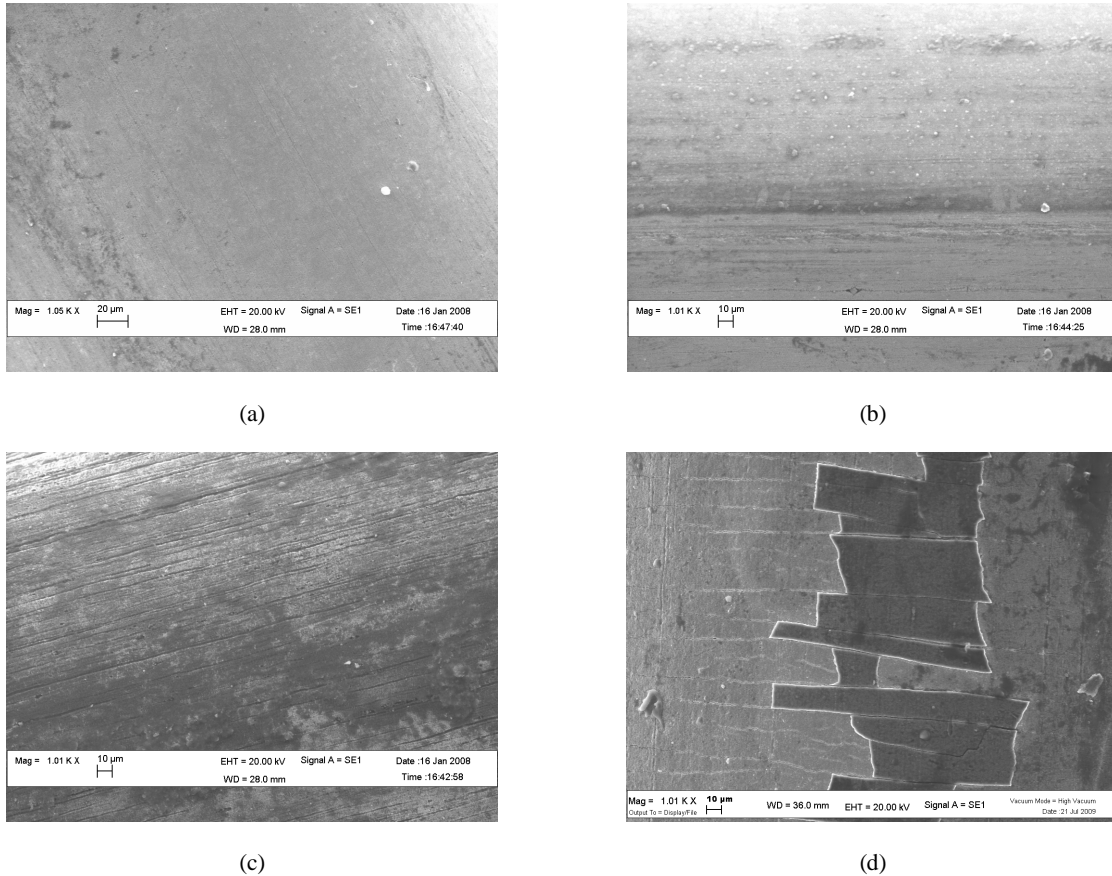
Figure 3.9: Surface of the wires after the treatment: (a) NT; (b) A; (c) AB; (d) S.

4 Conclusion

This work was a preliminary study to design a shape memory alloys adaptative composites.

In order to have a good response during activation and the recovery of original configuration the mechanical matrix and the surface adhesion between wires and matrix have been studied.

Two different thermoset resins have been considered and tested to choose the matrix with the tougher behavior and that have also the strength to re-strain the wire at the end of the activation.

The VE resin has a tougher behaviour than the PE resin according the 3-point bending test and that could ensure the recovery of the shape after the deformation caused by the wires actuation remaining in the elasticity region of the material.

At the same time the wire were subjected to 4 different superficial treatments to reach the maximum adhesion with the matrix and comparison were made with the pull-out test.

The use of the silane coupling agents can increase the adhesion strength more than the other etching treatment and this effect was observable with both matrices.

References

[1]   K. Otsuka, C.M Wayman, Shape memory materials Cambridge University Press Cambridge UK 1998.

[2]   K. Lau, A.W. Chan, S. Shi, L. Zhou, Debond induced by strain recovery of an embedded NiTi wire at a NiTi–epoxy interface: micro-scale observation, Mater. Des. 23 (2002) 265.

[3]   N.A. Smith, G.G. Antoun, A.B. Ellis, W.C. Crone, Improved adhesion between nickel–titanium shape memory alloy and a polymer matrix via silane coupling agentsCompos., Part A Appl. Sci. Manuf. 35 (2004) 1307.

[4]   D.C. Lagoudas, I.G. Tadjbakhash, Active flexible rods with embedded SMA fibers, Smart Mater. Struc. 1 (1992) 162.

[5]   Y. Furuya, A. Sasaki, M. Taya, Enhanced Mechanical Properties of TiNi Shape Memory Fiber/Al Matrix Composite, Mater. Trans., JIM 34 (1993) 224.

[6]   D.A. Hebda, M.E. Whitlok, J.B. Ditman, S.R. White, Manufacturing of Adaptive Graphite/Epoxy Structures with Embedded Nitinol Wires, J. Intell. Mater. Syst. Struct. 6 (1995) 220.

[7]   Z.G. Wei, R. Sandstrom, A. Miyazaki, Review shape memory materials and hybrid composites for smart systems, J. Mater. Sci. 33 (1998) 3763.

[8]   R. Prabhakaran, T.L. Galloway, Strain measurement in a shape memory alloy with strain gauges, Strain 41 (2005) 177.

[9]   K.A. Tsoi, R. Stalmans, J. Schrooten, Transformational behaviour of constrained shape memory alloys, Acta Mater. 50 (2002) 3535–3544.

[10] M. Tawfik, B. Duan , J. Ro, C. Mei, Suppression of post-buckling deflection and panel flutter using shape-memory alloy, The SPIE 7th International Symposium on Smart Structures and Materials, March 2000, 2000.

[11] K. Lau, AW.Chan, S. Shi, L. Zhou, Debond induced by strain recovery of an embedded NiTi wire at a NiTi–epoxy interface: micro-scale observation, Mater Des 2002;23:265–70.

[12] C. Poon, K. Lau, L. Zhou. Design of pull-out stresses for prestrained SMA wire/ polymer hybrid composites. Compos Part B: Eng 2005;36(1):25.

[13] S. Rossi, F. Deflorian, A. Pegoretti, D. D'Orazio and S. Gialanella Chemical and mechanical treatments to improve the surface properties of shape memory NiTi wires. Surface & Coatings Technology 202 (2008) 2214–2222

[14] P. Roche, L. El Medawa, J.-C. Hornez, M. Traisnel, J. Breme, H.F. Hildebrand, Biocorrosion and cytocompatibility assessment of NiTi shape memory alloys, Scr. Mater. 50 (2004) 255.

[15] J.S.N. Paine, W.M. Jones, C.A. Rogers, AIAA; 33rd Structural Dynamics and Materials Conference, 1992, p. 556.

[16] B.K. Jang , T. Kishi Adhesive strength between TiNi fibers embedded in CFRP composites, Materials Letters 59 (2005) 1338– 1341.

[17] M.F. Chen, X.J. Yang, Y. Liu, S.L. Zhu, Z.D. Cui, H.C. Study on the formation of an apatite layer on NiTi shape memory alloy using a chemical treatment method Man, Surf. Coat. Technol. 173 (2003) 229.

[18] M. Pohl, C. Heßing, J. Frenzel, Electrolytic processing of NiTi shape memory alloysMaterials Science and Engineering A 378 (2004) 191–199

[19] A.J. Kinloch, Adhesion and adhesives: science and technology, Chapman & Hall, London (UK), 1987.

[20] A.J. Kinloch, Adhesion and adhesives: science and technology, Chapman & Hall, London (UK), 1987.

[21] C. Trigwell, T. Duerig, Effects of surface treatment on the surface chemistry of NiTi alloy for biomedical applications, Surf. Interface Anal. 15 (1990) 349.

[22] Y. Payandeh, F. Meraghni,, E. Patoor , A. Eberhardt, Debonding initiation in a NiTi shape memory wire–epoxy matrix composite. Influence of martensitic transformation Materials and Design 31 (2010) 1077–1084.

[23]	B. Gabry, F. Thiebaud, C. Lexcellent, Topographic Study of Shape Memory Alloy Wires Used as Actuators in Smart Materials, J. Intell. Mater. Syst. Struct. 11 (2000) 592.

[24	SY Fu, CY Yue, X Hu, YW Mai. Analyses of the micromechanics of stress transfer in single-and multi-fibre pull-out tests. Compos Sci Technol 2000;60:569–79.

[25]	K. Jonnalagadda, G.E Kline, N.R Sottos. Local displacement and load transfer in Shape memory alloy composites, Experimental Mechanics, vol 37 n 1 March 1997 (78-86)

[26]	Li-Min Zhou, Yiu-Wing Mai, L. Yie,Analysis of fibre push-out test based on the fracture mechanics approach Compos. Eng. vol 5 n°10-11 (1995) pp 1199-1219.

[27]	J. S. N. Paine, C. A. Rogers, Adaptive structures and material systems AD-35 ASME New York (1993) 63–70.

[28]	M. R. Piggott, Failure processes in the fibre-polymer interphase Comp. Sci. Technol. 42(1) (1991) 57-76.

[29]	S. Zhandarov, E. Pisanova, On the mechanism of failure in microcomposites consisting of single glass fibers in a thermoplastic matrix, Compos. Sci. Technol. 57 (1997) 957-964.

[30]	A. J. Kinloch, Adhesion and adhesive: science and technology, Chapman & Hall, London (UK), 1987

[31]	EP Plueddemann, Silane coupling agents, Plenum Press, New York (USA), 1991.

ACKNOWLEDGMENTS